Advances in Thermal Processes and Energy Transformation
Volume 2, 2019, Heck01, p. 43-47
ISSN 2585-9102

Conditions Characterizing Hydrate Formation

● Dávid Hečko[1] ● Milan Malcho[2] ● Pavol Mičko[3] ● Peter Durčanský[4]

[1]*Department of Power Engineering, Faculty of Mechanical Engineering, University of Žilina, Veľký diel, 010 26 Žilina, Slovakia, david.hecko@fstroj.uniza.sk*
[2]*Department of Power Engineering, Faculty of Mechanical Engineering, University of Žilina, Slovakia, milan.malcho@fstroj.uniza.sk*
[3]*Department of Power Engineering, Faculty of Mechanical Engineering, University of Žilina, Slovakia, pavol.micko@fstroj.uniza.sk*
[4]*Department of Power Engineering, Faculty of Mechanical Engineering, University of Žilina, Slovakia, peter.durcansky@fstroj.uniza.sk*

Category : Original Scientific Paper
Received : 25 October 2019 / Revised: 30 October 2019 / Accepted: 31 October 2019

Keywords: accumulation, natural gas, hydrate, energy source, hydrate formation.

Abstract: For countries with limited access to conventional hydrocarbon gases, methane hydrates appear to be a potential source of energy. Given the demands of the European Union to reduce the energy intensity of technological processes, it shows as a prospective accumulation of natural gas and biomethane in the form of hydrate structures and, if necessary, release them. Storing gas in such a form creates an energy-efficient interest in developing and innovating technology in this area. However, the question arises: "How artificially accumulate methane energy into synthetically generated hydrates and practically implement it when needed?" Finding her answer is a current challenge in processes and technologies where energy needs to be stored.

Citation: Hečko D. et al: Conditions Characterizing Hydrate Formation, Advance in Thermal Processes and Energy Transformation, Volume 2, No.3 (2019), pp. 43-47, ISSN 2585-9102

1 Introduction

We are currently at a very early stage in the development of methane hydrates. The transition from scientific theory to practical extraction is under way. Developments for viable energy-efficient recovery are currently feasible, but the potential of this new hydrocarbon source is undeniable. The main reason is the storage capacity of hydrates compared to other natural gas treatments (CNG, LNG). Therefore, they are being considered as a potential source of energy for the coming decades [1,2].

For countries that do not abound in traditional gas reserves or rich shale forms, these hydrates are seen as a lifeline - as an example, Japan is leading them in their research.

2 Conditions for hydrate formation

Hydrates are generally solid crystalline substances formed by the combination of water and hydrocarbon gas molecules. These include methane, ethane, carbon dioxide and hydrogen sulphide. The article will focus on clathrate bonds of water and the most used energy carrier in the gas industry, namely natural gas [3].

Hydrates of natural gas and other similar compounds are classified by arranging the water molecules in the crystal and thus the crystal structure of the lattice. Due to hydrogen bonds, water molecules are often organized into three-dimensional spherical structures called cages. The second molecule is located inside the cage and stabilizes the entire structure.

The following table defines the necessary pressure and temperature at which hydrate methane structures will be formed [4].

The chemical composition of the aqueous phase and the hydrate is expressed as a molar percentage of methane and for the vapor is expressed as a molar percentage of water.

It can be seen in the graph that for the ethane, propane and isobutane contained in the hydrate mixture it was a function of temperature or pressure (i.e. they are constant). The reason for this is that the hydrate structure is occupied by large cavities and the large

cavities have a high occupancy rate. The values given in the tables are essentially 100% saturation values.

Table 1 Methane hydrate formation conditions

Temperature (°C)	Pressure (MPa)	Substance quantity (mol%)		
		CH_4	H_2O	CH_4
		Water	Steam	Hydrate
0,0	**2,60**	**0,10**	**0,027**	**14,1**
2,5	**3,31**	**0,12**	**0,026**	**14,2**
5	**4,26**	**0,14**	**0,026**	**14,3**
7,5	**5,53**	**0,16**	**0,025**	**14,4**
10	**7,25**	**0,18**	**0,024**	**14,4**
12,5	**9,59**	**0,21**	**0,024**	**14,5**
15	**12,79**	**0,24**	**0,025**	**14,5**
17,5	**17,22**	**0,27**	**0,025**	**14,5**
20	**23,4**	**0,30**	**0,027**	**0,025**

The means for the aqueous phase, steam and, if any, non-aqueous liquid were calculated using the available software. The chemical composition of the hydrate is estimated from the combination of the experiment data, computer software and crystalline hydrate structure.

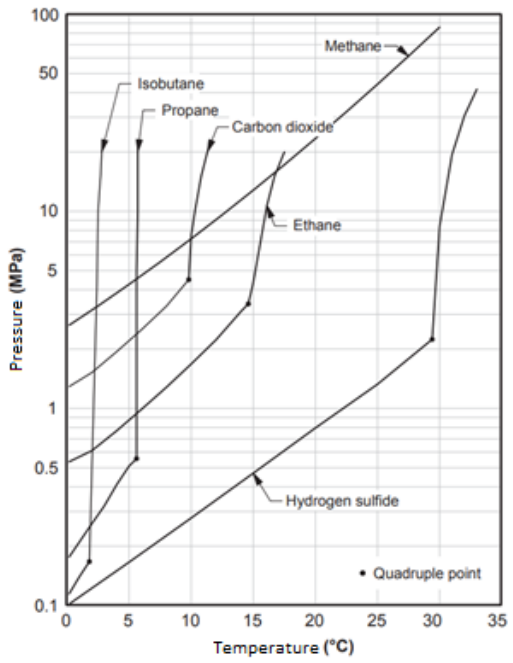

Figure 1 Conditions characterizing the formation of hydrate structures for several constituents present in natural gas [4]

For example, methane appears to be the most soluble of these hydrocarbons. The above values show significantly higher concentrations in the aqueous phase. However, solubility is a function of temperature and pressure. Methane is soluble at higher pressures compared to other hydrocarbons [4].

3 Generation of synthetic natural gas hydrates

The following part of the thesis deals with the description of the existing equipment in order to create suitable conditions for the accumulation of gas into hydrate structures. The design of the device was based on foreign studies, theoretical. The apparatus was designed based on these temperature and pressure conditions, a temperature of 0°C to 20°C and a pressure of 25 MPa. Given that temperatures below 0°C would lead to freezing of excess water to hydrates, it is recommended to form hydrates at temperatures just above zero [5]. The determination of the optimum temperature will depend on the results of experimental measurements.

The hydrate formation process was based on the patented system of two high pressure vessels. In the first vessel, the methane is hydrated and then pumped into the second vessel, where the capture and dehydration process takes place, i.e. removal of excess water from the mixture. Removal of excess water from the mixture is important to reduce the total volume of the resulting hydrate.

The production of methane hydrates is conditioned by the formation of contacts between the liquid and the gas. Therefore, the method of injecting water droplets into the gas continuous phase was chosen. In an aqueous continuous system, due to the high heat capacity of the water, the heat generated during hydrate formation can be effectively dissipated in the aqueous component, but a large amount remains unchanged. The injection of water into the gas at the stage of their interaction causes the formation of hydrates. This phenomenon occurs in two phases: nucleation and embryo growth. During nucleation, methane gas is dispersed in the aqueous component. Dissolved methane in water forms the seeds of hydrates and crystallizes. In the growth phase, the embryos formed are sized or aggregated. The shape and size of the nozzle plays an important role in this process, since the shape of the droplets or their surface depends on it [6].

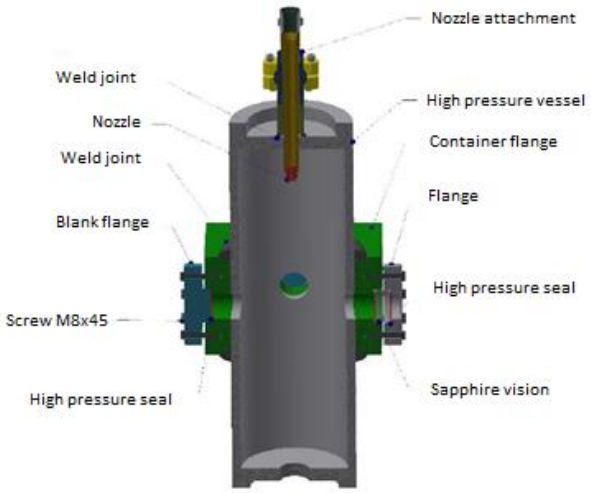

Figure 2 Location of the injection nozzle

The water and gas will be mixed in the pipeline just prior to supply to the first 5.7 litre main pressure vessel. The water / gas mixing ratio is 1/150 to 1/170. At the inlet to the container, the water will be sprayed by means of a nozzle. Spraying the liquid into small particles will facilitate the process of enclosing the gas into the water grid. In the design we consider two alternatives - nozzles with a spray angle of 55° and 150°. We assume that in practice a solution with a larger spray angle will prove to be more effective as it can cover a wider area with small particles of water [7].

4 Measuring and recording technology

The measurement of the required temperature and pressure parameters will be provided by means of sensors with electronic output for measuring temperature (NiCrNi thermocouples and Pt100 sensors) and pressure. The output is connected to the ALMEMO 5690-2 AHLBORN control panel and is connected to a computer. Data is written according to a specified time cycle in Excel. The NiCrNi thermocouple consists of two different metals welded at one end, where a thermoelectric voltage is generated as a function of temperature. The Pt100 resistor works on the principle of changing the electrical resistance depending on the temperature change of the sensor.

The experimental device has been innovated over time and has undergone many design changes to the final form shown in the *Figure 2*.

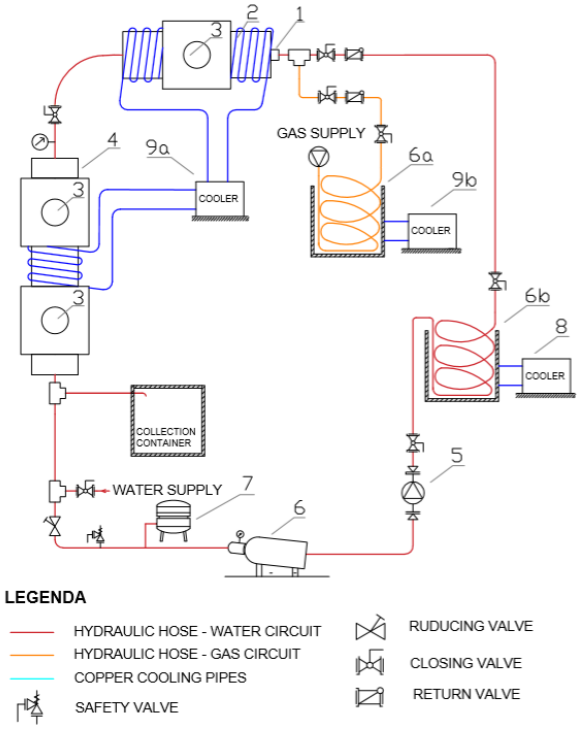

Figure 2 Wiring diagram of the experimental device

Table 2 Schematic positions on the experimental device

	Part of device	**Model/type**
1	Nozzle	Spray angle 51°/ 155°
2	Vessel VN1	φ175/146,9 mm,
3	Sapphhire visor	Normal φ 50 mm
4	Vessel VN2	Ø 175/146,9 mm
5	Plunger pump	P = 4,7 kW
6	Accumulator	Volume 20l,working pressure 207bar
6a	Cooling container	Plastic material
6b	Cooling container	Plastic material
7	Expansion tank	Working pressure 16 bar
8	Cooler	Q=60 $l.min^{-1}$, p_{max}= 6bar
9a/9b	Cooler	Q=11-16 $l.min^{-1}$, p_{max}= 0,45bar

The measurement methodology on the experimental device consisted of the following steps. First, the entire system is cooled to the desired temperature by actuating the cooling devices. The cooling process takes about 3 hours. Before the start of the measurement, the entire system is filled with water through the water inlet. When the system is filled with water, the gas branch opens. Compressed gas starts to push the water towards the pump suction while monitoring the level to drop to half the sapphire visor on the VN1 vessel. Further, the natural gas pressure will be increased to the desired value for measurement, e.g. to 120 bar. After reaching the desired pressure, the gas branch is closed. A high-pressure pump 5 is actuated to circulate the water and methane solution through the atomizing nozzle in the experimental apparatus. From this point on, a hydrate will be formed over time.

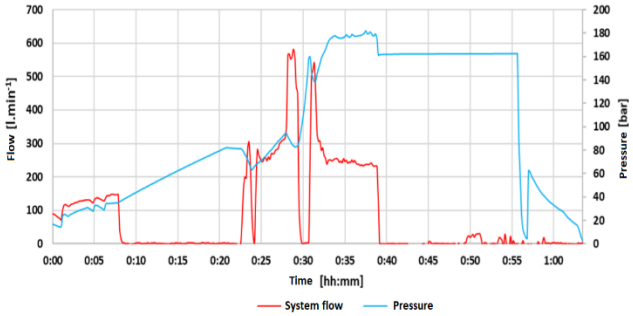

Figure 3 Flow and pressure measurement

The whole process is graphically depicted as a function of pressure over time. The measurement took about 1 hour and 4 minutes. At this time, the gradual filling of the natural gas system is included, followed by the displacement of water from the VN1 vessel to the visible part of the sapphire visor (the pressure in the graph rises; , within about 35 minutes). At 38 minutes, pump 6 was switched on, which maintained a nearly constant pressure for about 55 minutes. Then the pressure dropped sharply, which was probably due to water being absorbed into the hydrate structure and thus lack of water at the pump suction.

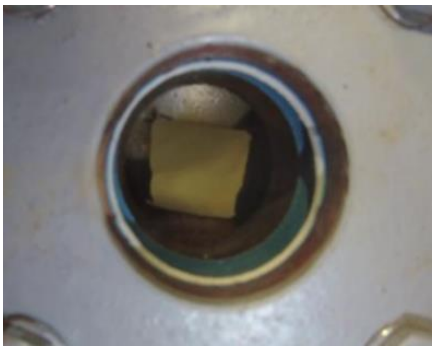

Figure 4 Recording of the hydrate formed

The *Figure 4* shoes the hydrate formed in the VN2 pressure vessel, at the bottom of the vessel.

In the measurement, natural gas consumption was 2,187 m^3, hydrate formation time of 2:00 minutes and an average pressure of 97 bar. Based on a subjective visual assessment and average pressure value, the hydrate structure appears to be perspective.

5 Conclusion

Hydrates of natural gas or methane have an interesting potential and therefore the future energy demand from hydrocarbon sources may be a requirement to improve synthetic hydrate formation processes. A prospective option is to accumulate standard natural gas in the form of artificially formed hydrates, with subsequent storage and, where necessary, covering energy peaks with future release. Gas can be stored in such a form at relatively high temperatures and low pressures compared to other hydrocarbon gas storage technologies.

Hydrates can become a current challenge for the future and, once verified, can find application in various sectors of technology or industry. A particular solution is appropriate to apply in the technology industry to cover energy-intensive peaks in cogeneration and trigeneration, e.g. with the option of using waste heat to heat and then release stored energy when necessary.

The reference list

[1] FOLTIN, V., RAJZINGER, J.: '*Natural gas hydrate – Challenge and Opportunity'*, Infront Outback – Conference – Zborník príspevkov z 32. Stretnutia katedier mechaniky tekutín a termomechaniky, pp. 45-48, 2013.

[2] RAJZINGER, J., RIDZOŇ, F., KIZEK, J., FOLTIN, V., KNÍŽAT, B.: *Comparative study of selected thermodynamic derivate properties of methane for isenthalpic and isothermal throttling and isentropic processes.* In: The application of experimental and numerical methods in fluid mechanics and energy 2014: 19. International Scientific Conference, Nizke Tatry, pp. 207-2012, 2014

[3] HARRISON, E. S.: *Natural gas hydrate*, Standford University, [Online], Available: <http://large.stanford.edu/courses/2010/ph240/harrison1/> [24 Oct 2010], 2010.

[4] CARROL, J. 2014.: *Natural gas hydrates a guide for engineers*, 3rd edition, Gulf Professional Publishing, Waltham, 2014.

[5] Mitsubishi Heavy Industries. 2002. *Gas hydrate production device and gas hydrate dehydrating device*, [online], 2002, Available: www.google.com/patents/US2005010 7648

[6] PAVLENKO, A.M., KOSHLAK, H.V., USENKO, B.O. 2014.: *Basic principles of gas hydrate technologies*. Thermal technology, metal journal publishing, 2014.

[7] MALCHO M., LENHARD R., KADUCHOVÁ K., *Energy storage in to the hydrates*, In: AIP Publishing, Volume 2000, Article number 020014, 2018.

Acknowledgement

Work on article has been financially supported by the project VEGA-1/0738 / 18 „Optimization of energy inputs for the rapid generation of natural gas and biomethane hydrates for the accumulation of high potential primary energy“ and the project KEGA-063ŽU-4/2018 „Depositing hydrocarbon gases into hydrate structures as an alternative energy storage method.“

Advances in Thermal Processes and Energy Transformation
Volume 2, 2019, Mick01, p.48-51
ISSN 2585-9102

Thermal Comfort Measurement for Wet Floor Cooling System

Pavol Mičko[1] ● Andrej Kapjor[2] ● Dávid Hečko[3] ● Marián Pafčuga[4]

[1]Department of Power Engineering, University of Žilina, Univerzitná 1, 010 26 Žilina, Slovakia, pavol.micko@fstroj.uniza.sk
[2]Department of Power Engineering, University of Žilina, Univerzitná 1, 010 26 Žilina, Slovakia, andrej.kapjor@fstroj.uniza.sk
[3]Department of Power Engineering, University of Žilina, Univerzitná 1, 010 26 Žilina, Slovakia, david.hecko@fstroj.uniza.sk
[4]Department of Power Engineering, University of Žilina, Univerzitná 1, 010 26 Žilina, Slovakia, marian.pafcuga@fstroj.uniza.sk

Category : Original Scientific Paper
Received : 22 October 2019 / Revised: 28 October 2019 / Accepted: 29 October 2019

Keywords : Radiant floor cooling, Thermal comfort, Heat-humidity microclimate

Abstract : The trend of constant increase in energy prices can be observed especially on the increased demands on the thermal insulation properties of building structures of buildings. According to European Directive 2010/31 / EU, since 2019 only buildings that meet the energy standards of near zero buildings have to be designed. In practice, the design of the building takes into account, in particular, the shape of the building, its cladding, but also the method and technology for heating, cooling and hot water production. In the case of a family house is considered a specific annual consumption of heat for heating up to 20 kW.h.m^{-2} floor area. A popular way to achieve low heat consumption is to select an efficient heat source - a heat pump. It is best to combine a heat pump with a heating system with a low temperature gradient. The combination of heat pump and radiant floor heating is very popular. Modern heat pumps also come with the possibility of reversible operation and serve as a source of cold. The following article will therefore address floor radiant cooling and its effect on thermal comfort.

Citation: Mičko P., et.al: Thermal Comfort Measurement for Wet Floor Cooling System, Advance in Thermal Processes and Energy Transformation, Volume 2,No. 3 (2019), p. 48-51, ISSN 2585-9102

1 Introduction

From 2010 to 2019, the increase in heat prices is more than 45% [4]. This forces users to look for economical heating and cooling systems. At the same time, legislation prescribes the design of buildings with minimum heat losses and thermal loads. European Directive 2010/31 / EU makes it impossible to issue a building permit for buildings that do not fall into categories A1 and better. One of the ways in which a building can meet these conditions is to choose the appropriate method and technology for heating, cooling and hot water production. Many new buildings use the heat pump as the heat source. In combination with radiant underfloor heating, it seems to be the most advantageous solution from fully-automated heating systems in terms of operating costs. A considerable disadvantage is the higher purchase costs. However, this disadvantage can be compensated by the versatility of the heat pump and the possibility of use not only as a heat source but also as a source of cold, where the cooling system can also be an existing floor heating distribution.

2 Cooling using a radiant floor system

The cost of the heat pump is significantly higher than that of a gas condensing boiler. However, if one source is used for both heat and cold production, the total purchase price is consequently lower than for one specific heat source and a separate cold source. Most heat pumps can also operate in reversible mode and can produce cold. A simple circuit diagram of the heat pump so that it can serve as a heat source in winter but also as a source of cold in summer and can also produce hot water is shown in Fig. 1.

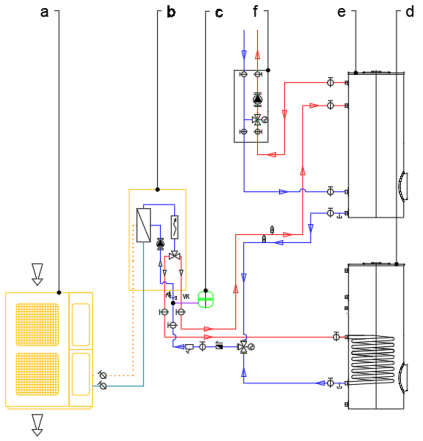

Figure 1 Heat pump wiring diagram for heating and cooling - a) External heat pump unit, b) Internal heat pump unit, c) Expansion vessel, d) Domestic hot water tank, e) Buffer vessel, f) Pump group.

This system is able to replace cooling systems with minimal investment costs in the summer months. However, the performance of a cooling device is limited by several factors that limit its use. When used in combination with a floor radiant system, a suitable temperature gradient should be considered because of the risk of condensation of water vapor on the cooled surface of the structure. An unfavorable factor is also the elimination of the influence of natural convection and accumulation of cold air above the floor. These facts can have a major impact on thermal comfort and comfort in a cold room [6].

3 Thermal comfort for floor cooling

The most important environmental component, the thermal-moisture microclimate, is used to assess the appropriate thermal condition of interiors - thermal comfort. Its disruption affects homoiothermia. A person with his / her mental and physical state is able to adapt to a certain microclimate. There is a range (neutral zone) in which the adaptation requirements are minimal and the person feels best there. In this state, one does not feel cold or resp. excessive heat. The state of thermal comfort can be expressed as a function of six independent variables (thermal comfort factors) [1,2,5].

$$f(q_q, R_{cl}, \theta_i, p_i, v_i, \theta_u) = 0 \qquad (1)$$

q_q - total density of heat flow from the human body ($q_q = q_m \pm q_w$) [W.m^{-2}]
R_{cl} - thermal resistance of clothing [m^2.K.W^{-1}] ([CLO])
θ_i - indoor air temperature [°C]
p_i - partial pressure of the water vapor of the internal air [Pa]
v_i - Indoor air flow rate [m.s^{-1}]
θ_u - Average radiant temperature [°C]

The first two parameters characterizing the state of thermal comfort and thus qq and Rcl are subjective. These parameters vary from user to user. The other four parameters are objective and physical-measurable quantities determining the state of the environment [1].

3.1 Measurement in a thermostatic chamber

For accurate determination of boundary conditions for measuring the thermal comfort of floor cooling, measurements were carried out in a thermostatic chamber for testing and evaluating the performance of heating elements and convectors according to EN 442 part 2. The length of the chamber is 4 ± 0.02 m, width 4 ± 0.02 m height 3 ± 0,02 m. During cooling, cooling water with a flow temperature of 17 ° C flows through the floor system. This temperature is limiting because of local thermal discomfort in the foot area but also because of the risk of water vapor condensation on the floor. Fluorescent lamps are used as the thermal load of the building, which converts 99% of electrical energy into heat. The lamps are evenly distributed over the corners of the room in a total of 12 pieces. The indoor air temperature is controlled by the superior system to maintain the equilibrium conditions and the reference room temperature is in the range of 26 ± 0.5 ° C. With the known fluorescent lamp power, 520 W or the known flow and temperature gradient of the cooling water, we can accurately determine the cooling power during equilibrium in a thermostatic chamber. The parameters of the indoor air temperature-humidity microclimate were measured at five stations according to the following Fig. 2.

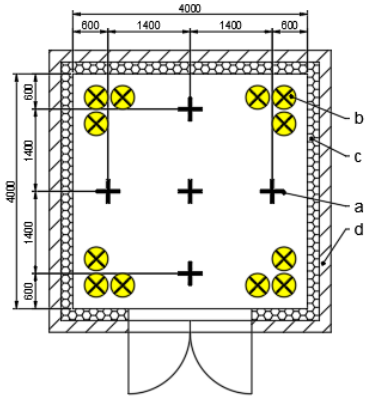

Figure 2 Plan view of thermostatic chamber - a) the position of the measurement of the thermal-humidity microclimate, b) the electric lamp - thermal load, c) the thermal insulation, d) construction of the thermostatic chamber.

3.2 Measuring device

To measure the thermal comfort in the thermostatic chamber, we used the ComfortSense device from Dantec Dynamics. The measuring elements of the device comply with EN 13 182, ISO 7726 and ISO 7730 standards. Overall, the device had five measuring elements. Three measuring elements were used to measure the indoor air temperature and air flow rate. The first, T1, was placed at a height of 0.1 m from the floor and thus at the height of the ankles. The second element, T2, was placed at a height of 1.1 m, the center of gravity of the body. The third element, the T3, was positioned at head level, 1.7 m from the floor. The fourth, OT element, with an ellipsoid shape, is used to measure the operating temperature (function of the effective temperature of the surrounding surfaces). The last element, RH, is used to measure the water vapor partial pressure of the indoor air and assess the relative humidity of the room air. The measuring probes are located on a common tripod of Fig. 3 so that measurements can be made at each station indicated in the thermostatic chamber top view of Fig. 2.

Figure 3 ComfortSense measuring device [3]

3.3 Measured parameters of thermal-humidity microclimate

All objective parameters of the thermo-humidity microclimate was measured during equilibrium in a thermostatic chamber where the average temperature of all sensors was 26 ± 0.5°C. The remaining objective parameters were chosen according to the estimation of the anticipated activity or the value according to the norm was chosen. The selected total heat flux density from the human body was a standing, slightly active user, where production is expected to be 90-100 $W.m^{-2}$. The thermal resistance of the clothing for measuring the thermal comfort of cooling systems is set at 0.5 CLO, or 0.078 $m^2.K.W^{-1}$. Table 1 shows the average values of the measured variables from all the stations, even with the measurement uncertainty.

Table 1 Average parameters of thermal-humidity microclimate for floor cooling

Measuring element	T1	T2	T3	OT	RH
Indoor air flow rate [$m.s^{-1}$]	**0,02 ±0,02**	**0,02 ±0,02**	**0,02 ±0,02**		
Indoor air temperature [°C]	**25,18 ±0,2**	**27,08 ±0,2**	**27,27 ±0,2**		
Operative temperature [°C]				**25,77 ±0,2**	
Relative humidity [%]					**39,51 ±2**

4 Evulation of Thermal comfort in floor cooling

For the assessment of the environment, we can use the seven-stage psychophysical scale by Gage, Stolwijk and Hardy:

-3 - cold, -2 - cool, -1 - slightly cool, 0 - neutral, +1 - slightly warm, +2 - warm, +3 - hot.

The resulting thermal status of the measured environment by Petráš (2005) is expressed using the Predicted Mean Vote (PMV), which results in the average value of the thermal sensations of a large group of users. The PMV index reflects the average sense of well-being of a large group of users, but feeling of individual's can move around the resulting value. For this reason, the PPD (Predicted Percentage of Dissatisfied) was used to express the predicted percentage of people dissatisfied with the thermal environment. An environment in which the PPD of 5% to 10% is optimal for the human body [1].

Tab. 2 shows the PMV and PPD values for a wet floor cooling system with a heat load stabilized at 520 W. These values are shown in the graph of PPD and PMV indices in Fig. 4

Table 2 PMV and PPD values for a wet floor cooling system

Measuring element	T1	T2	T3
PMV [-]	**-0,33**	**-0,12**	**-0,11**
PPD [-]	**7,21**	**5,32**	**5,24**

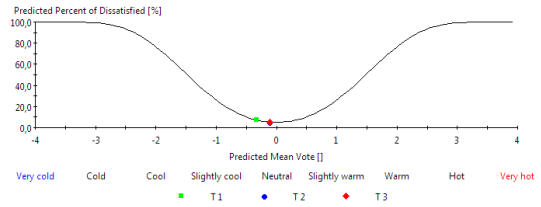

Figure 4 Dependence of PPD and PMV indices for wet floor cooling

A simpler idea of indoor air temperature distribution, as well as vertical and horizontal temperature gradients, is illustrated in Fig. 5. In the figure we can observe the gradual distribution of temperatures in the vertical direction due to the absence of a significant proportion of the convective component in the distribution of cold in the room.

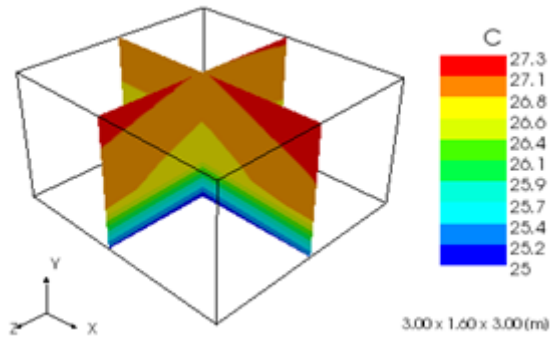

Figure 5 Temperature distribution in the interior for wet floor cooling

4 Conclusions

The return of the heat pump can be significantly reduced in its use as a source of cold. In combination with a wet floor radiant system it forms a frequent and comfortable combination for heating buildings. With a suitable design, it can replace the cooling system with minimal purchase costs. However, the condition of low heat load of the building must be taken into account. The maximum thermal load for an area of 16 m^2 in the thermostatic chamber where the measurement was carried out at equilibrium was 520 W. The floor surface was formed by concrete screed. In normal use, however, the floor surface will be a laminate floor, ceramic tile or other surface material. Thus, it can be determined that under normal conditions the cooling power of the system is at most 30 $W.m^{-2}$. Such outputs are only sufficient for passive houses and houses with low thermal loads. Assessment of the environment and the thermal-moisture microclimate in the thermostatic chamber where the cooling system of the measurements represented a PPD index interval of 〈 5.24; 7.21〉, representing a range of nearly 2%. The wet floor cooling system can therefore be evaluated as comfortable and at the same time affordable. However, local thermal comfort factors must also be taken into account, as a long stay on the cold floor can lead to discomfort.

Reference list

[1] PETRAS, D.: *Vykurovanie rodinných a bytových domov*, Bratislava, Jaga group, 2005.

[2] SZÉKYOVÁ, M., FERSTL, K., NOVÝ, R.: *Vetranie a klimatizácia*, Bratislava, Jaga group, 2004.

[3] DANTEC DYNAMICS.: ComfortSense, [Online], Available: https://www.dantecdynamics.com/comfortsense [3 December 2019], 2019.

[4] ZILINSKA TEPLARENSKA.: Ceny tepla, [Online], Available: http://www.teplarenzilina.sk/dokumenty/ceny-tepla# [3 December 2019], 2019.

[5] RESEARCHGATE.: Practical evaluation of the thermal comfort parameters, [Online], Available: https://www.researchgate.net/publication/305755583_Practical_evaluation_of_the_thermal_comfort_parameters [3 December 2019], 2002.

[6] PAPUCIK, S., NOSEK, R., LENHARD, R.: *Vykurovanie*, Žilina, EDIS, 2012.

Acknowledgement
This article was supported by project APVV-15-0778 “Limits of Radiative and Convective Cooling through the Phase Changes of Working Fluid in Loop Thermosyphon”, APVV-15-0790 “Optimalization of biomass combustion with low ash melting temperature” and KEGA 033ŽU-4/2018 “Heat sources and pollution of the environment”,

Advances in Thermal Processes and Energy Transformation
Volume 2, 2019, Pand02, p.52-56
ISSN 2585-9102

Secondary Ways of Nitrogen Oxides Reduction

Iveta Pandová[1]

[1]*Department of Process Technique, Technical University of Košice, Faculty of Manufacturing Technologies with a seat in Prešov, Bayerova 1, 080 01 Prešov, Slovak Republic, iveta.pandova@tuke.sk*

Category : Original Scientific Paper
Received : 16 September 2019 / Revised: 27 September 2019 / Accepted:28 September 2019

Keywords : combustion, nitrogen oxides, reduction, catalyst

Abstract : Nitrogen oxides are combustion pollutants that play an important role in many atmospheric processes that affect climate change, ecosystem stability and population health. Their occurrence is highest in industrial and densely populated areas. Nitrogen oxides undergo chemical reactions in the atmosphere, leading to a greenhouse effect and global warming. The paper contains an overview of reactions in which nitrogen oxides are involved in atmosphere, as well as an overview of methods for nitrogen oxides emissions reducing into the environment.

Citation: Pandová Iveta: Secondary Ways of Nitrogen Oxides Reduction, Advance in Thermal Processes and Energy Transformation, Volume 2, Nr.3 (2019), p. 52-56, ISSN 2585-9102

1 Introduction

Nitrogen oxides play an important role in many atmospheric processes with strong implications for ecosystem stability, climate change and public health. Nitrogen oxides are produced in large quantities by combustion, primarily in the form of NO, which is oxidized to NO_2. In a lower atmosphere, nitrogen oxides contribute to the formation of acid rain, as well as to the formation of ozone and aerosol. In addition, nitrogen oxides are toxic at high concentrations. In higher atmospheric layers, nitrogen oxides contribute to the decomposition of the ozone layer [1]. The most important nitrogen oxides are N_2O, NO, NO_2.

2 Reactions of the Nitrogen Oxides at Atmosphere

Small particles and gases are emitted daily into the atmosphere by industrial activity, internal combustion engines, energy production, building heating, agricultural activity. The monitored gases also include nitrogen oxides. More than 90% of the nitrogen oxides are from internal combustion engines emitted in the form of nitric oxide (NO), which in the stratosphere is oxidized to nitrogen dioxide (NO_2). It has a negative effect on the respiratory tract of living organisms. NO_2 emissions destroy the ozone layer and also represent greenhouse gas causing climate change. Excessive occurrence of NO_2 in the troposphere leads to an undesirable increase in the concentration of tropospheric ozone. The following reactions occurring in the troposphere are sources of ozone [2,3]:

$$O_2 + h.\upsilon\ (< 242\ nm) \rightarrow O + O \quad (1)$$

$$NO_2 + h.\upsilon\ (< 400\ nm) \rightarrow NO + O \quad (2)$$

$$O_2 + O + M \rightarrow O_3 + M \quad (3)$$

The neutral collision particle (M) balances the energy ratios of the reaction. Increased ozone concentration in the troposphere, causes diseases of the respiratory tract and nervous system. Nitrogen oxides from the flue gases of the supersonic aircraft reach the stratosphere, where N_2O reacts with atomic oxygen to form nitric oxide, which reacts with ozone, thereby contributing to the depletion of the ozone layer in the atmosphere [3].

$$N_2O + O \rightarrow 2NO \quad (4)$$

$$NO + O_3 \rightarrow NO_2 + O_2 \quad (5)$$

$$NO_2 + O \rightarrow NO + O_2 \quad (6)$$

The following equation expresses the resulting reaction.

$$O_3 + O \rightarrow 2O_2 \quad (7)$$

Nitrogen oxides and volatile organic compounds react in the presence of sunlight to produce photochemical smog, a significant form of air pollution. The presence of photochemical smog increases in summer when the incident solar radiation is higher. Hydrocarbons emitted from industrial activities and transport react with NO_x rapidly and increase the concentration of ozone and peroxide compounds, in particular peroxyacetyl nitrate [4]. Children and people with lung diseases such as asthma, are particularly sensitive to the adverse effects of smog, which causes damage to lung tissue and decreased lung function. Nitrogen dioxide is also involved in the formation of nitric acid and acid rain. NO_2 is oxidized in the gas phase during the day by reaction with a hydroxyl radical.

$$NO_2 + HO (+ M) \rightarrow HNO_3 (+ M) \quad (8)$$

M is the molecule required to stabilize the addition product. Nitric acid (HNO_3) is highly soluble in liquid water in aerosol particles or in clouds [5]. NO_2 also reacts with ozone to form a nitrate radical [5].

$$NO_2 + O_3 \rightarrow NO_3 + O_2 \quad (9)$$

During the day, the NO_3 radical rapidly undergoes photolysis, but at night it can react with the NO_2 molecule to form nitric oxide.

$$NO_2 + NO_3 (+ M) \rightarrow N_2O_5 (+ M) \quad (10)$$

N_2O_5 reacts rapidly with liquid water (in aerosol particles or in cloud drops, but not in the gas phase) to form nitric acid.

$$N_2O_5 + H_2O \rightarrow 2HNO_3 \quad (11)$$

The reaction is considered to be the major route of nitric acid formation in the atmosphere [5]. Nitric acid contributes to acid rain or can be deposited in soil where it generates nitrates which are taken up by plants. The reaction in the aqueous phase is too slow to have any significance in the atmosphere [5].

$$2NO_2 + H_2O \rightarrow HNO_2 + HNO_3 \quad (12)$$

3 Methods for Reducing Nitrogen Oxides

Emission regulations for unburned hydrocarbons, nitrogen oxides and particulate matter are increasingly stricter worldwide. Transport (mobile source) and fuel combustion (stationary source) are the main sources of nitrogen oxide emissions [6]. Power generation, stationary engines, industrial boilers, process heaters and gas turbines are the main stationary sources of NOx [2]. Several technologies have been applied to reduce nitrogen oxide emissions from both stationary and mobile sources .Methods of reducing nitrogen oxides in flue gases are divided into primary and secondary. The primary measures adjust the combustion process to produce the lowest NOx content. Secondary measures reduce the already formed NOx from flue gas. These are divided into wet and dry. Wet methods utilize absorption into solutions. Sodium hydroxide is most commonly used as an absorbent. This process proceeds according to the following reactions:

$$NO + NO_2 + 2NaOH \rightarrow 2NaNO_2 + H_2O \quad (13)$$

$$2\ NO_2 + 2NaOH \rightarrow NaNO_2 + NaNO_3 + H_2O \quad (14)$$

The dry processes include adsorption and reduction methods. The most commonly used techniques for reducing nitrogen oxides are:

a) non-catalytic reduction
b) catalytic reduction
c) wet cleaning

In the non-catalytic reduction of a mixture of nitrogen oxides and ammonia, nitrous oxide is converted to elemental nitrogen and water vapor at temperature interval 800ºC - 1000ºC according to the equations [7]:

$$6\ NO + 4\ NH_3 \rightarrow 5\ N_2 + 6\ H_2O \quad (15)$$

$$6\ NO_2 + 8\ NH_3 \rightarrow 7\ N_2 + 12\ H_2O \quad (16)$$

In the catalytic reduction of the mixture of nitrogen oxides with methane, carbon monoxide and hydrogen, the oxides of nitrogen are converted to nitrogen, carbon dioxide and water according to the equations: [7]:

$$4\ NO + CH_4 \rightarrow 2\ N_2 + CO_2 + 2\ H_2O \quad (17)$$

$$2\ NO_2 + CH_4 \rightarrow N_2 + CO_2 + 2\ H_2O \quad (18)$$

$$2\ NO + 2\ CO \rightarrow N_2 + 2\ CO_2 \quad (19)$$

$$2\ NO_2 + 4\ CO \rightarrow N_2 + 4\ CO_2 \quad (20)$$

$$2\ NO + 2\ H_2 \rightarrow N_2 + 2\ H_2O \quad (21)$$

$$2\ NO_2 + 4\ H_2 \rightarrow N_2 + 4\ H_2O \quad (22)$$

According to literature, SNCR technology is currently the best available technology that meets the required level of environmental protection [2]. Selective reduction is achieved by reaction with aqueous ammonia or urea solution according to the reactions:

$$4\ NH_4OH + 2\ NO + 2\ O_2 \rightarrow 3\ N_2 + 10\ H_2O \quad (23)$$

$$CO(NH_2)_2 + 2\ NO + ½\ O_2 \rightarrow 2\ N_2 + CO_2 + 2\ H_2O \quad (24)$$

he reaction proceeds either at temperatures of about 850°C in the combustion chamber of the boiler without catalyst, but with lower efficiency, or at about 350°C on the surface of the catalyst with high efficiency. Thus, from a chemical point of view, denitrification can be catalytic or non-catalytic. Particular attention is paid to selective catalytic reduction with an emphasis on catalysts for the reduction of NO from stationary sources. The catalyst is needed due to the high activation energy of the direct decomposition reaction. The reducing agent is injected in front of the catalyst, which then gives rise to events which can be described by reactions [2]:

$$4\ NO + 4\ NH_3 + O_2 \rightarrow\ 4\ N_2 + 6\ H_2O \quad (25)$$

$$NO + NO_2 + 2\ NH_3\ \rightarrow\ 2\ N_2 + 3\ H_2O \quad (26)$$

The most commercial devices use a V_2O_5/TiO_2 catalyst, although there are many devices that use zeolite technology [6]. V_2O_5 levels also play a role in minimizing SO_3 formation [4]. In addition, modifiers such as Mo and W are added to improve the long-term performance of the device [4]. Introducing an additional reductant in the exhaust of combustion process can circumvent the thermodynamic and kinetic difficulties in reducing NOx. By selectively promoting the reaction of NOx with a reductant over the reaction of NOx with O_2, SCR catalysts can achieve NOx concentrations that are below the thermodynamic equilibrium concentration [9]. However, the reaction mechanism of selectively reducing NO is complicated and still not well understood because of the many side reactions occurring between different proportions of NO, NH_3, and O_2 across different temperatures. Set of reactions was observed by Wang et. al. over a Cu-V/γ-Al_2O_3 catalysts[10].

$$6\ NO + 4\ NH_3 \rightarrow 5\ N_2 + 6\ H_2O \quad (27)$$

$$4\ NO + 4\ NH_3 + O_2 \rightarrow 4\ N_2 + 6\ H_2O \quad (28)$$

$$2\ NO_2 + 4\ NH_3 + O_2 \rightarrow 4\ N_2 + 6\ H_2O \quad (29)$$

$$4\ NO + 4\ NH_3 + 3O_2 \rightarrow 4\ N_2O + 6\ H_2O \quad (30)$$

$$2\ NH_3 + 5/2\ O_2 \rightarrow 2\ NO + 6\ H_2O \quad (31)$$

$$2\ NH_3 + 2\ O_2 \rightarrow N_2O + 6\ H_2O \quad (32)$$

$$2\ NO + O_2 \rightarrow 2\ NO_2 \quad (33)$$

$$2\ N_2O + 3O_2 \rightarrow 4\ NO_2 \quad (34)$$

$$2\ NH_3 + 3/2\ O_2 \rightarrow N_2 + 3\ H_2O \quad (35)$$

SCR systems need to be constantly improved in the light of the gradual tightening of emissions regulations. Their performance can be improved by adjusting the various processes that occur in these complex systems. Computational Fluid Dynamics (CFD) provides a cost-effective means to achieve more efficient NOx conversion by the SCR system. SCR systems usually consist of multiple catalyst layers. The results of the study show a significant effect of the second catalyst layer on the overall performance of the SCR system. The second catalyst layer plays an important role in the reduction of NOx as well as ammonia [8].

4 Catalyst Processes Utilizing Zeolites

Dry catalyst processes include processes utilizing surface-treated sorbents, for example zeolites after incorporation of metal elements such as Co, Pt, Cu. Various catalytic materials have been investigated, and both the carrier and the catalyst component have been shown to be critical for degradation at a lower operating temperature. These catalysts, such as Co / Beta zeolite, are deposited on a ceramic support and accelerate the reduction of nitrogen oxides to nitrogen.
The use of zeolite materials finds application especially in mobile sources. According to recent research, the most effective method appears to be SCR catalyzed by a zeolite catalyst. Superior activity and selectivity of a Cu ion-exchanged SSZ-13 zeolite in the selective catalytic reduction (SCR) of NO_x with NH_3 were observed, in comparison with Cu-beta and Cu-ZSM-5 zeolites. Cu-SSZ-13 was not only more active in the NO_x SCR reaction over the entire temperature range studied (up to 550°C), but also more selective toward nitrogen formation, resulting in significantly lower amounts of NO_x by-products (i.e., NO_2 and N_2O) than the other two zeolites. In addition, Cu-SSZ-13 demonstrated the highest activity and N_2 formation selectivity in the oxidation of NH_3. The results of this study strongly suggest that Cu-SSZ-13 is a promising candidate as a catalyst for NO_x SCR with great potential in after-treatment systems for either mobile or

stationary sources [11]. More recently, Cu^{2+}-exchanged beta zeolite (Cu-beta) has been shown to have excellent activity in the SCR of NO_x with NH_3, and metal-exchanged beta zeolites are generally found to have greater hydrothermal stability than similar ZSM-5 catalysts . In the very recent patent literature, Cu^{2+} ion-exchanged SSZ-13 (Cu-SSZ-13) has been reported to exhibit NO_x conversions of 90–100% over a wide temperature range in the NH3-SCR process, and its activity exceeded 80% even after extensive high-temperature hydrothermal aging [12]. The SSZ-13 zeolite has chabazite (CHA) structure with a relatively small pore radius (~3.8 Å) in an eight-membered ring [13]. Copper ions were exchanged into the zeolite in an aqueous ion-exchange process[11].The activity and selectivity of the Cu-SSZ-13 catalyst for both NO_x SCR with NH_3 and NH_3 oxidation are superior to those of both Cu-beta and Cu-ZSM-5 . The Cu-SSZ-13 catalyst maintains its high conversion (>90%) up to 500 °C, while the NOx conversion of Cu-ZSM-5 begins to decline above 300 °C [11]. The order of high-temperature NH_3 SCR reactivity is the inverse of the order in pore size, i.e., SSZ-13 having the smallest pores (~4 Å, 8-membered ring) being the most active, ZSM-5 with medium size pore opening (~5.5 Å, 10-membered ring) having medium activity, and beta with the largest pores (~7 Å and ~5.5 Å, 12-membered ring) having the lowest activity [11]. Under the same reaction conditions for NO_x SCR with NH_3, Cu-SSZ-13 demonstrates superior activity and N_2 formation selectivity in comparison with Cu-beta and Cu-ZSM-5 zeolites [11].

5 Conclusion

Nowadays, as environmental problems are increasingly important, it is particularly important to reduce emissions of gaseous substances that not only harm health but also contribute to the greenhouse effect and global warming. Such gaseous substances also include nitrogen oxides. Therefore, the efforts of scientific teams are constantly improving the equipment for reducing nitrogen oxides. Currently, the best available technology is SNCR technology. The efforts of scientific teams are to improve this technology, but also to introduce new technologies. In particular, the combination of catalytic conversion with sorption is promising. Suitable sorbents are zeolites with incorporated metal cations which influence the reaction of the conversion of nitrogen oxides to nitrogen catalytically. Currently, the combination of SCR technology with zeolites is mainly used in mobile sources.

6 The reference list

[1] CASTELLANOS, P., FOLKERT BOERSMA, K : Reductions in nitrogen oxides over Europe driven by environmental policy and economic recession. [Online],Available: https://www.ncbi.nlm.nih.gov/ pmc/articles/PMC3280598/ [16. Feb.2012] 2012.

[2] HEIDE, B.: *Best Avaible Technology (BAT) for NOx Reduction in Waste to Energy Plants*, Mehlday & Steinfath Umwelttechnik GmbH, 2008.

[3] HORBAJ, P.:Vznik oxidov dusíka a ich vplyv na rozpad ozónovej vrstvy. *Chem. Listy* 91, pp. 833 – 839, 1997.

[4] WARNECK, P. *Chemistry of the natural atmosphere.* San Diego: Academic Press.Vol.71, 927, 2000.

[5] SEINFELD, J., PANDIS, H.; SPYROS, N.: *Atmospheric Chemistry and Physics: From Air Pollution to Climate Change.* Hoboken, New Jersey: John Wiley & Sons, 2006.

[6] M HECK, R.: Catalytic abatement of nitrogen oxides–stationary applications: *Catalysis Today*, Vol. 53, Issue 4, pp .519 -523, 1999.

[7] HORBAJ P.: *Ekologické aspekty spaľovania* 1999.

[8] OGIDIAMAA, O. V., SHAMIM, T.: Investigation of Dual Layered SCR Systems for NOx Control. *Energy Procedia* 75, pp. 2345 – 2350, 2015.

[9] GORALSKI, C.T. Jr. SCHNEIDER,W.F.: Analysis of the thermodynamic feasibility of NOx catalysis to meet next generation vehicle NOx emissions standars. *Applied Catalysis B: Environmental* 37, 263–277,2002.

[10] WANG, CHENGIUN., ZUO, YUENGANG., YANG, CHEN-LU: Selective Catalytic Reduction of NO by NH_3 in Flue Gases over a Cu-V/Al_2O_3 Catalyst at Low Temperature, *Journal of Engineering Science*, 9, 2009.

[11] JA HUN KWAK RUSSEL, G., TONKYN DO HEUI KIM., SZANYI, J. ,PEDEN, Ch.H.F.: Excellent activity and selectivity of Cu-SSZ-13 in the selective catalytic reduction of NO_x with NH_3. *Journal of Catalysis* , Vol. 275, Issue 2, pp. 187-190, 2010.

[12] BULL, I., XUEW. M., BURK, P., BOORSE, R.S.,JAGLOWSKI, W.M.,

OERMER,G.S.,MOINI, A..PATCHET, J.A., DETTLING J.C., CAUDLE,M.T. : US Patent7,610,662, 2009.

[13] ZONES, S. I.: US Patent 4,544,538, 1985.

Acknowledgement

This article was supported by the state grant agency for supporting research work and co-financing the project KEGA 004TUKE-4/2018 and by the Development Agency under the contract No. APVV-16-0192.

.

Advances in Thermal Processes and Energy Transformation
Volume 2, 2019, Past01, p. 57-60
ISSN 2585-9102

Design of Equipment and Methodology for Secondary Tar Removal after Gasification in Low Heat Output Generators

Marcel Pástor[1] ● Ladislav Lukáč[1] ● Gustáv Jablonský[1] ● Filip Furka[1]

[1]*Department of Thermal Engineering and Gas Industry, Faculty of Materials, Metallurgy and Recycling, Institute of Metallurgy, Technical university of Košice, Letná 9, 042 00 Košice, Slovakia,*
marcel.pastor@tuke.sk, ladislav.lukac@tuke.sk, gustav.jablonsky@tuke.sk

Category : Original Scientific Paper
Received : 22 October 2019 / Revised: 30 October 2019 / Accepted: 31 October 2019

Keywords : filter, gasification, tar, wood chips

Abstract : This paper described tar formation and its removal methods. There are analysed at the base on measurements realized on the department of heat engineering and gas industry by gasifying of wood pellet and wood chips for a gasification reactor. It is proposed a dry method to tar removing with the cascade configuration filtration cartridges.

Citation: Pástor M.,et. al: Design of Equipment and Metodology for Secondary Tar Removal after Gasification in Low Heat Output Generators, Advance in Thermal Processes and Energy Transformation, Volume 2, No.3 (2019), pp. 57-60, ISSN 2585-9102

1 Introduction

The most important technical measures for achieving air pollution reduction include reducing emissions from individual sources to the surrounding atmosphere.

During the gasification of the fuel after its drying (below 150°C), pyrolysis occurs to remove volatile combustible material. Biomass thermal pyrolysis products are process gas, tars and pyrolysis coke. The pyrolysis gas partially burns and the released heat is consumed to run the endothermic reduction reactions to form CO, CO_2, CH_4 and H_2, which are the main component of the generated gas in gasification with air [1].

The resulting generator gas can be combusted in gas turbines or in cogeneration piston combustion engines.

2 Wood biomass gasification

2.1 Fuel used during gasification

The basis for stoichiometric calculation is elementary fuel composition (Table 1). The fuel components affect the thermal efficiency and heat loss of the fuel conversion equipment.

Table 1 Average elemental composition of incoming wood biomass used for experimental gasification reactor (% by weight)

Composition %	Type of fuel	
	Chips	Pellets
Ash	0,67	0,4
C	46	50,3
H	5,56	5,7
O	39,5	33,05
N	0,27	0,22
S	0	0,03
Moisture	8	10
Calorific value, MJ/kg	16,84	17,5

In the thermochemical conversion of biomass, the input moisture of the fuel most judged is the value of which varies depending on the source of fuel, the season and the storage conditions. For some types of equipment, it is necessary to pre-dry the fuel, which increases input costs.

2.2 The experimental updraft gasifier

The measurements were performed on an experimental updraft gasification reactor with an expected 15 kW heat output. The composition and fuel consumption, the amount and enrichment of the gasification air (atmospheric air - pure oxygen mixture), the backfill level of the fuel layer in the reactor and their effect on the amount and quality of the generator gas produced were monitored. After stabilization of the reactor temperature, samples of the produced gas were taken for analysis 20 cm from the reactor outlet.

Taken samples were analysed by absorption analysis. The CO_2, O_2, CO content was determined, followed by combustion and re-absorption of the CO_2 and CH_4 concentrations, and the H_2 concentration was determined. The residual gas is considered pure N_2. In the analysis, it was considered that all hydrocarbons in the gas phase were in the form of CH_4.

The biomass is fed to the top of the updraft gasification reactor. Air is fed under the grate. The flue gas (1000°C) passes upwards, supplying heat to the endothermic gasification reactions, cooling to 200°C - 300°C at the top of the reactor.

Typical wood gas composition is 40 – 50 % N_2, 15 – 20 % H_2, 10 – 15 % CO, 10 – 15 % CO_2 and 3 – 5 % CH_4, its calorific value is 4 - 6 MJ/m^3, if pure oxygen is used with water vapour, increases to 10 -18 MJ/m^3. Applying the process of gasification on the solid biomass, mainly the waste wood in form of wood chips, achieved is the transformation of the solid combustible biomass into the gaseous fuel - wood gas. This can than be utilised in the system of the combined electricity and heat production (Figure 1). The gasifying process takes place in the counterflow type gasifier, operating on the solid bed [2].

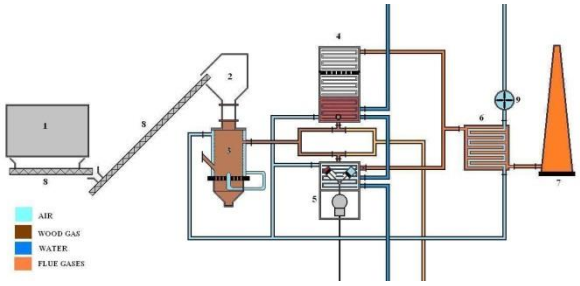

Figure 1 Scheme of low power cogeneration equipment for solid biomass [2]
1- wood-chip storage, 2- hopper, 3- updraft gasifier, 4-hot-water boiler, 5-cogeneration unit, 6-heat exchanger, 7- chimney, 8- conveyor, 9-exhaust fan

The wooden material is supplied into the gasifier, where the thermochemical transformation takes place. The needed heat for the gasification process is supplied by the partial wood combustion. The product of the process operating on air is the wood gas. The main combustible component is hydrogen, carbon monoxide, methane, hydrocarbons and also non-combustible products. This gas is afterwards burned in the CHP unit - thermal engine with the resulting heat and electricity generation. With regard to the properties of the polluted wood gas, it is necessary to apply specially modified thermal engine. Expected electricity output of the CHP unit is 35 kWe.

The sensitive heat of waste gas from the thermal engine will be in the economiser recuperated into the heating water. To balance the non-uniformity in heat consumption, proposed is the hot water boiler operating on the wood gas from the solid biomass gasification [2].

3 Formation of tar and removing them

When air is used as a gasifying medium, the resulting high N_2 content doubles the volume of wood gas. In order to achieve a higher calorific value of the gas, the moisture content of the input fuel should be less than 15 – 20 %, so that it is usually required to pre-dry it where waste heat from the engine can be used. The energy content of the gas produced is up to 75 % of the biomass energy content [3].

The main contaminants of raw wood gas are the particulate matter (soot, dust) and tar. Wood gas may also contain other impurities, namely ammonia (which is converted to NO_x during combustion engine), HCl, H_2S, alkalis and acids [4].

Primary tar is produced at relatively low temperatures (200-500°C). It is a mixture of condensed hydrocarbons. The average value of tar produced by the steam utilization is 30 - 80 g.m^{-3}, steam/air mixture 4 - 30 g.m^{-3} and air 2 - 20 g.m^{-3}. Tar removal is very important in cases where the produced gas is cooled or compressed before use and in mechanical systems such as internal combustion engines or gas turbines

The average tar concentration of the experimental measurements in the raw wood gas is 50 g.m^{-3}. Therefore, it is necessary to implement primary or secondary methods to reduce the tar content of wood gas.

The most commonly used primary methods are the optimum gasification operating conditions, the addition of additives/catalyst (dolomite, K_2CO_3, Na_2CO_3, Al_2O_3) to the gasifier bed and the gasification plant itself [5].

Secondary methods are mechanical separation and thermal or catalytic cracking. The separate tar destruction and reforming reactor is used. Wet and hot gas is cleaned.

With OLGA technology, aerosols, heavy and light tars with a specially developed cleaning agent are delivered to the absorption column. Dust - free gas is required, a hot gas filter is used.

3.1 The draft of filter device

A separate experimental device (Figure 2) was created to monitoring tar formation. The weighed amount of wood chips was placed in a gasification tube (Figure 2), sealed with a flange, and inserted into an electrical resistance oven (Figure 3). There are two inlets on the front of the gasifier, the air needed to the fuel gasification through the bottom, and the gas produced through the filter on the torch, where it is combusted.

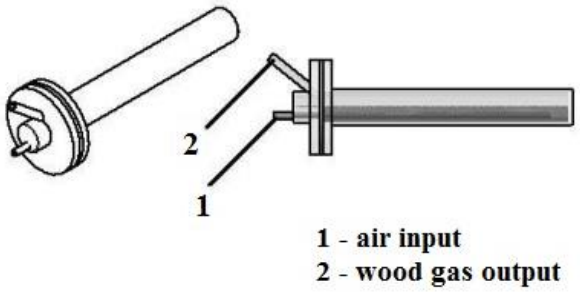

Figure 2 The experimental gasifying device

Figure 3 The electrical resistance oven

The furnace temperature is controlled by a potentiometer with a range of 100°C by 1200°C. Dust particles and condensed tars (already at 300°C) are trapped on the filter. With a charge weight of 17 – 20 g and airflow of 1dm^3.min^{-1}, the gas flow is so slow that it is not necessary to cool the gas. The measurement results are shown in Table 2.

Table 2 Measurement results for tar formation

measurement	1	2	3	4
fuel	wood chips			
moisture (w. %)	25		0	
gasifying (min)	15		9,2	10
air excess	0,25			
charge (g)	15	15	9,5	9,8
gasifying temperature (°C)	770	870	770	870
air amount (dm^3)	15	15	9,2	10
weight of captured components (g)	3,5	2,8	1,8	1,9

Based on the obtained results, a filtering device was designed and constructed (Figure 4), which supplemented the basic experimental scheme (Figure 5) [6,7].

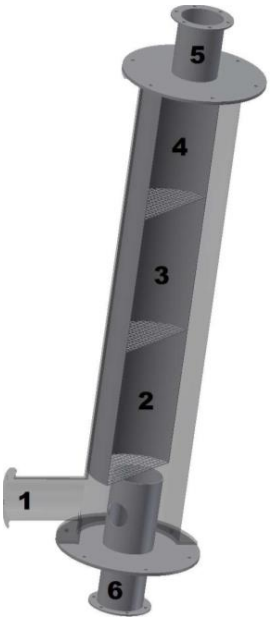

1 - gas input
5 - gas output
2, 3, 4 - filter cartridges
6 - condensate output

Figure 4 The filter device design [6]

The wood gas enters the filter at the bottom and flows upward through the filter material. The outgoing gas passes through the pipe to the combustor torch.

After removing the lower part of the filter, the filter material, which is stored in the containers - is inserted into the filter cartridge. The filter height is 110 cm and the tube diameter is 180 mm.

The filter cartridges are three with a diameter of 170 mm and a height of 30 cm. It is possible to give different kinds of filter material to each cartridge, or use their mixtures. Glass beads with a diameter of 2

cm, wood chips and wood pellets were used as filter material [6].

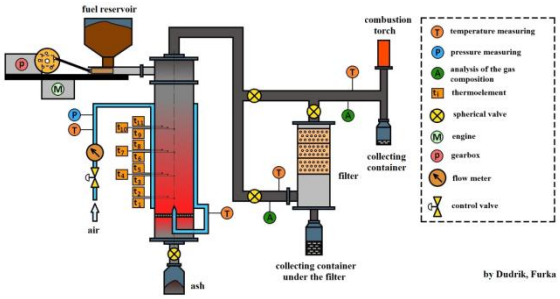

Figure 5 Scheme of the filter device with measuring points [6]

For correctly operation of the device, the following procedure has been proposed for practical measurements:

1. Visual inspection of the gasification generator, filtering equipment and the conveyor path - inspection of the measuring points, check of the functionality of the ball valves and checking the tightness of the filtering device.
2. Cleaning - begins with the dismantling of the bottom of the gasification reactor, followed by cleaning of the grate from unburned parts of the fuel from the previous experiment, control, resp. removing stickers formed around the periphery of the gasifier generator and checking the nozzle functionality.
3. Ignition - a small amount of fuel is supplied to the grate, which is ignited by the gas burner. By monitoring the temperature, the supply of fuel and gasification air slowly increases to the required amount.
4. Temperature stabilization in the reactor. The total rise and stabilization time of the gasification process is 1.5 to 2.5 hours. A steady state is taken when the temperature difference does not change by more than 20°C within 10 minutes.
5. After steady-state temperatures have been reached in the reactor, samples of the generated gas are taken. The measurement ends by weighing the last measured weight of the filter cartridge, disconnecting the gasification air and terminating the fuel addition. Fuel pyrolysis and partial cooling of the whole plant are partly taking place.

The efficiency of the filtering device is determined by the ability to separate the mixture of tar, dust particles and water vapour from the product gas.

4 Conclusions

It is important to consider stick formation of condensed hydrocarbons for all types of gasification equipment. The formation of tar and removing them reduces the efficiency of thermal equipment. Cascading arrangement of filter cartridges it allows flexible exchange during the process. The adjustment of the filter material depends on the type of used fuel and the gasification conditions.

5 The reference list

[1] YANG, H., YAN, R., CHEN, H., LEE, H., D., ZHENG, CH.: Characteristics of hemicellulose, cellulose and lignin pyrolysis, *Fuel*, Vol. 86, Issues 12–13, pp. 1781-1788, 2007.

[2] LUKÁČ, L.: Výroba tepla z biomasy pre vybraný objekt, *Plynár - Vodár - Kúrenár + Klimatizácia*, Vol. 15, No. 1, pp. 12-13, 2017.

[3] DHYANI, V., BHASKAR, T.: A comprehensive review on the pyrolysis of lignocellulosic biomass, *Renewable Energy*, Vol. 129, Part B, pp. 695-716, 2018.

[4] KNOEF, H.: Handbook Biomass Gasification. BTG, Netherlands, 2005.

[5] KAN, T., STREZOV, V., EVANS, J., T.: Lignocellulosic biomass pyrolysis: A review of product properties and effects of pyrolysis parameters, *Renewable and Sustainable Energy Reviews*, Vol. 57, pp. 1126-1140, 2016.

[6] KOČANOVÁ, S., JABLONSKÝ, G., FURKA, F., LUKÁČ, L., SZÉPLAKY, D., NALEVANKOVÁ, J.: Draft of filtering device for experimental updraft Gasifier reactor, Quaere 2014: Recenzovaný sborník příspěvků vědecké interdisciplinární mezinárodní vědecké konference doktorandů a odborných asistentů, Vol. 4, Hradec Králové, Česká republika, pp. 1653-1661, 2014.

[7] FURKA, F.: *Filtračné zariadenie pre protiprúdny splyňovací generátor nízkeho výkonu*, Metalurgia Junior 2013, Košice, pp. 154-157, 2013.

Acknowledgement
This publication is the result of the Project implementation: Research centre for efficient integration of the renewable energy sources, ITMS: 26220220064 supported by the Research & Development Operational Programme funded by the ERDF.